CHAPTER 4

RIVER HYDRODYNAMICS

Rivers and streams are natural open channels with a free surface as a streamline along which the pressure is constant and equal to atmospheric pressure (Sturm 2001). The existence of a free surface means that the flow boundaries are no longer fixed by the channel geometry but adjust themselves to accommodate the flow conditions. Another aspect of open channel flow is the wide variability of the cross-sectional shape and roughness of the channel. Due to the free surface, gravity, instead of pressure, is the driving force, as in closed conduits (Sturm 2001).

The flow of water in natural channels is almost always unsteady (Mahmood and Yevjevich 1975). The unsteady nature of open channel flow causes the complexity of its analysis. The procedure one follows to predict the temporal and spatial variations of a flood wave as it traverses a river reach or reservoir is known as flood routing (Baltas 1988).

Advanced mathematical treatment of unsteady flow in open channels began with the development of two partial differential equations published in the Transactions of the

French Academy of Sciences, Volume 73, July-December 1871, presented by Barre de Saint-Venant. The English title of this document was "Theory of unsteady water flow, with application to river floods and to the propagation of tides in river channels." The second part of this document, titled "Theory and general equations of unsteady flow in open channels," contained two partial differential equations currently known as the Saint-Venant partial differential equations of unsteady flow. These two equations have remained unchanged in their general form since they were first published, during which time many scientists and researchers attempted to modify or improve them. Although these attempts result in more complete and sophisticated versions of the equations, they reduce to the basic Saint-Venant equations upon simplification for practical use (Mahmood and Yevjevich 1975).

Saint-Venant, an engineer as well as a mathematician-physicist, realized that the properties of fluid phenomena, as discovered by observations in nature as well as obtained by experiments, should be the guiding factors in postulating basic hydraulic equations. The fundamental assumptions in the development of Saint-Venant equations can be listed as: (i) hydrostatic pressure distribution along the depth of the flow; (ii) friction losses in the unsteady flow are similar to those in steady flow (so that the Manning or Chezy equations can still be used to calculate the mean shear boundary stress (Sturm, 2001); (iii) velocity distribution does not affect wave propagation; (iv) the flow can be represented in one dimension with negligible transverse velocity and average boundary shear stress applicable to the whole cross-section; and, (v) the bed slope is

small enough so that the sinus of the slope angle can be replaced by the tangent of the angle (Mahmood and Yevjevich 1975; Sturm 2001).

4.1. Derivation of the Saint Venant Equations

The equations required for solving the velocity and depth distribution in any open channel are the conservation of momentum and mass equations, which make up the Saint-Venant equations. These equations can be derived using Reynold's transport theorem for the given cross-section of a river channel in Figure 4.1.

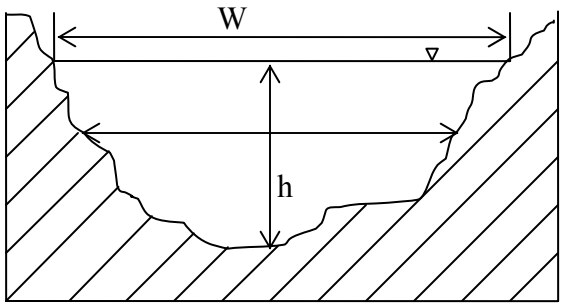

Figure 4.1 Cross-sectional view of a river channel.

The cross-sectional area of the channel as well as the top width of the channel changes with respect to the change in the water depth of the channel. The control volume of the system can be shown as in Figure 4.2.

Total mass and momentum have to be conserved within this control volume. (Streeter and Wylie 1979) present the general form of the conservation law for an arbitrary control volume, shown in Figure 4.2 as

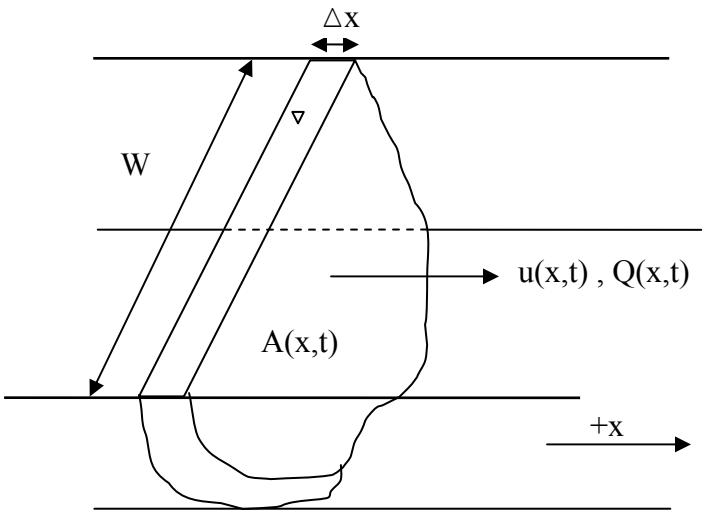

Figure 4.2 Control volume of a river cross-section

$$\frac{dB}{dt} = \iiint_{cv} \frac{\partial b}{\partial t} dV + \iint_{cs} b(\bar{u}\hat{n}) dA \tag{4.1}$$

where B is the system property, b is the intensive value of B per unit mass m, t [T] is time, V [L^3] is the volume of control volume (cv), $\bar{u}$ [L/T] is the velocity vector, $\hat{n}$ is the unit outward normal vector in the flow direction, and A [L^2] is the area of control surface (cs). By introducing different variables for B, one can derive the conservation of mass, momentum, and energy equations using Equation (4.1).

For mass conservation, *B* becomes mass [M] and b becomes the density (ρ) [M/L^3]. As mass cannot be created or destroyed, as stated by the first law of thermodynamics, the rate of change of mass term becomes zero, and the conservation of the mass equation is given as

$$0 = \iiint_{cv} \frac{\partial \rho}{\partial t} dV + \iint_{cs} (\rho \bar{u}.\hat{n}) dA \,. \tag{4.2}$$

For the momentum conservation, the storage term, becomes the total forces acting on the control volume, and the b value becomes the product of the velocity vector and the density as in

$$\overline{F} = \iiint_{cv} \frac{\partial \bar{u} \rho}{\partial t} dV + \iint_{cs} (\rho \bar{u}.\hat{n}) dA \,. \tag{4.3}$$

For incompressible fluids such as water, density does not change with time and through some algebra, Equation (4.2) can be written as Equation (4.4) below:

$$\frac{\partial A}{\partial t} + \frac{\partial Q}{\partial x} = 0 \,. \tag{4.4}$$

At any cross-section, the time rate of the change of the flow area due to the rise and fall of the free surface must be balanced by a spatial gradient of volume flux Q [L^3/T] in the flow direction. Equation (4.4) represents this situation (Sturm 2001).

The momentum equation equates the net force acting on the control volume with the time rate of change of the momentum in the control volume in addition to the rate of efflux of the momentum through the control volume. The resulting equation is given in Equation (4.5):

$$\begin{aligned} &\frac{\partial(Q\Delta x)\rho}{\partial t}+\rho\left\{\left[u(Au)\right]+\frac{\partial}{\partial x}\left[u(Au)\frac{\Delta x}{2}\right]\right\} \\ &-\rho\left\{\left[u(Au)\right]-\frac{\partial}{\partial x}\left[u(Au)\frac{\Delta x}{2}\right]\right\}=\overline{F} \end{aligned}, \tag{4.5}$$

where Q [L^3/T] is the flow rate, Δx [L] is the length of the river reach, ρ [M/L^3] is the water density, u [L/T] is the velocity, A [L^2] is the cross-sectional area, and $\overline{F}$ [L/T^2] is the total force acting on the control volume in the flow direction.

Force vector $\overline{F}$ can be expanded into three subcategories: gravity, shear, and pressure forces.

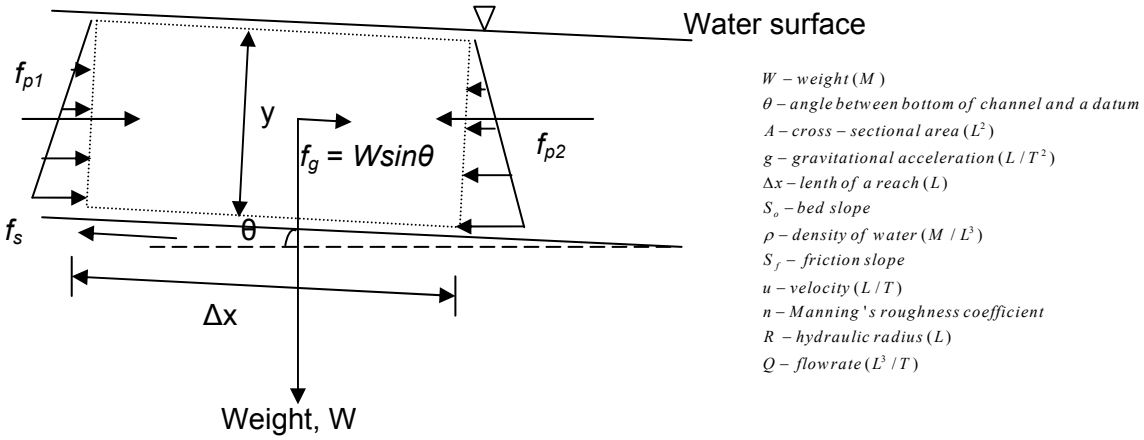

Figure 4.3 Forces acting on the control volume

The forces acting on the control volume are shown in Figure 4.3. Pressure forces act on either side of the control volume. Assuming hydrostatic pressure distribution, the net pressure force would be the difference between these two forces. The resulting difference is caused by the change in surface water elevations at each side of the control volume.

The gravitational force in the x-direction can be calculated using the component of the weight of the water in the x-direction. When angle θ is small enough, the sine and tangent of the angle become identical, and the tangent of the angle is the bed slope (i.e., $\rho g A \Delta x \sin\theta$, in which $\sin\theta$ is the bed slope S_0). Therefore, the gravitational force can be given as

$$f_g = W \sin\theta = \rho A g \Delta x \sin\theta \simeq \rho A g \Delta x S_o , \tag{4.6}$$

where W [ML/T^2] is the weight force, ρ [M/L^3] is the density, A [L^2] is the area, g [L/T^2] is gravitational acceleration, and Δx [L] is the length of the control volume.

Shear force f_S represents the depletion of momentum due to the action of friction on the sides and bottom of the channel. The shear force is mathematically analogous to the gravitational force, so it can be represented very similar to the gravitational force, the only difference between the two force equations is the slope term. In the shear force term, friction slope is used instead of the bed slope used in the gravitational force term:

$$f_S = \rho g A \Delta x S_f , \tag{4.7}$$

where S_f [L/L] is the friction slope, which can take any one of several forms, one of which uses Manning's equation:

$$S_f = \frac{u^2 n^2}{(c.R^{2/3})^2}, \tag{4.8}$$

where u [L/T] is the velocity of water, n is Manning's roughness coefficient, c is a unit system dependent constant (it is 1.0 in the SI unit system, and 1.486 in the British unit system), and R [L] is the hydraulic radius, given as the area divided by the wetted perimeter. When this definition of friction slope is introduced into the shear force in Equation (4.7), the shear force becomes

$$f_S = \rho g A \Delta x \frac{u^2 n^2}{(c.R^{2/3})^2} = \rho g A \Delta x \frac{n^2 |Q| Q}{c^2 . A^2 R^{4/3}} \tag{4.9}$$

Pressure force f_p, the total pressure force acting on the face of the control volume, is directly related to the change in the water depth along the channel:

$$f_p = -\rho g A \frac{\partial h}{\partial x} \Delta x . \tag{4.10}$$

The final form of the conservation of momentum equation becomes

$$\frac{\partial Q}{\partial t} + \frac{\partial}{\partial x}(Qu) + gA\frac{\partial h}{\partial x} = gA(S_0 - S_f), \tag{4.11}$$

where Q [L^3/T] is the flow rate, u [L/T] is the velocity, t [T] is the time, A [L^2] is the area, x [L] is the distance along the river, h [L] is the water surface elevation, g [L/T^2] is gravitational acceleration, S_0 is the bed slope, and S_f is the friction slope.

The continuity and the conservation of momentum equations together form the system of equations representing unsteady flow in channels known as the Saint-Venant equations. They are coupled, non-linear, first-order partial differential equations of the hyperbolic type. Their solution requires one initial and two boundary conditions. These equations have no analytical solution except in a few special cases.

The set of full, non-simplified forms of the original and the modified Saint-Venant equations are known as the dynamic wave model. The first term in Equation (8) is local acceleration, the second term is convective acceleration, the third term is the effect of gravity on the water surface slope, and the last term is frictional resistance.

4.2. Modifications to the Saint Venant Equations

The Saint-Venant equations form the basis of the general mathematical model of the unsteady non-uniform flow in channels; however, they need to be modified for application to natural systems such as rivers, as natural channels are significantly different from man-made channels in terms of channel geometry, channel bed roughness and river form. As a result, several researchers, including Fread (1976) and DeLong (1986 and 1989), have modified the Saint-Venant equations so that they can be applied in

natural channels. They have included the effects of complex channel geometry by adding flood-plains and a meandering pattern in the equations. Once modifications are applied, the Saint-Venant equations can more easily account for the effects of the flood plain, inactive (off-channel or dead) storage, and the meandering ratio (sinuosity factor) of the river (Gunduz and Aral 2004). Below, these modifications and changes in the form of the conservation and momentum equations are described as follows:

i. *Lateral flow.*

The first modification is the addition of lateral flow. In a natural river system, water can enter the system as surface runoff, referred to as *lateral overflow*. Some water in the system can also be lost to groundwater as seepage flow. Such flows affect both the conservation and momentum equations. Additional loss from the system, reflected in the conservation equation in the following form, may also occur:

$$\frac{\partial A}{\partial t} + \frac{\partial Q}{\partial x} = q_L \ , \tag{4.12}$$

where q_L , the lateral flow, can take two different forms:

$$q_L = q_{L_1} + q_{L_2} \, , \tag{4.13}$$

where q_{L1} is lateral overflow and q_{L2} is seepage outflow. As movement is involved in overland inflow and seepage outflow, the momentum equation also requires modification as follows:

$$\frac{\partial Q}{\partial t}+\frac{\partial (Qu)}{\partial x}=-gA\frac{\partial h}{\partial x}+gA(S_o-S_f)+M_L, \tag{4.14}$$

where the momentum effect of the overland flow and seepage flow can be separated again:

$$M_L = M_{L_1} + M_{L_2} \tag{4.15}$$

and each of the terms can be described in terms of flow and area as follows:

$$M_{L1}=\begin{cases} 0 & \text{for seepage inflow} \\ -\dfrac{Qq_{L1}}{2A} & \text{for seepage outflow} \end{cases} \tag{4.16}$$

$$M_{L2}=\begin{cases} -\beta \upsilon_x q_{L2} & \text{for overland inflow} \\ -\dfrac{Qq_{L2}}{A} & \text{for overland outflow} \end{cases} \tag{4.17}$$

where q_{L1} is the lateral seepage flow per channel length (positive for inflow and negative for outflow), q_{L2} is the lateral overland flow per channel length (positive for inflow and negative for outflow), β is the momentum coefficient for velocity distribution, g is gravitational acceleration, h_r is the water surface elevation in the river (i.e., stage), M_{L1} is the momentum flux due to lateral seepage inflow/outflow, and M_{L2} is the momentum flux due to lateral overland inflow/outflow.

ii. *Dead storage.*

In natural rivers, the geometry of the channel is not smooth, as it is in man-made channels. In general, portions of the river, typically near the banks of rivers, contain still water pools called dead storage, as they are not moving. These areas, shown in Figure 4.4, can be represented in Equation (4.18):

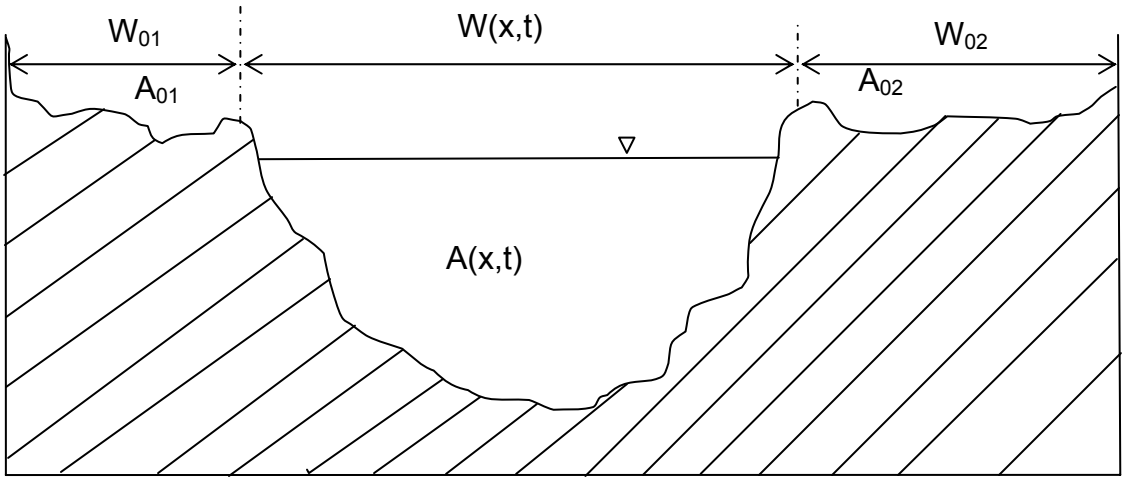

Figure 4.4 Dead storage in natural rivers

$$\frac{\partial(A+A_o)}{\partial t}+\frac{\partial Q}{\partial x}-q_L=0\,. \tag{4.18}$$

Since dead storage zones involve no movement only the mass conservation equation, not the momentum equation, is affected.

iii. *Channel constrictions.*

Natural channels typically experience some constrictions that cause head loss in the flow of water. Thus, head loss needs to be incorporated into the net force balance in the momentum equation. The head loss term is usually given as

$$f_{E/C} = -\rho g \Delta h_E , \tag{4.19}$$

where ρ is the density, g is gravitational acceleration, and Δh_E is head loss, which in turn is defined by the following equation:

$$h_E = \frac{K_E}{2g}\left(\frac{Q}{A}\right)^2 , \tag{4.20}$$

where K_E is the head loss coefficient, g is gravitational acceleration, Q is the flow rate, and A is the area. The head loss caused by constrictions in the river channel can be incorporated into the momentum conservation equation as a slope term, shown in Equation (4.21)

$$S_{E/C} = \frac{K_E \Delta (Q/A)^2}{2g\Delta x} . \tag{4.21}$$

Hence, the momentum equation becomes

$$\frac{\partial Q}{\partial t} + \frac{\partial (Qu)}{\partial x} = -gA\frac{\partial h}{\partial x} + gA(S_o - S_f - S_{E/C}) + M_L . \tag{4.22}$$

Since no additional loss of water from the river occurs, the mass conservation equation remains unaltered.

iv. *Momentum correction factor.*

In natural rivers, the velocity is substantially non-uniform across the width of the river. In order to compensate for the assumption of uniform velocity across the width of the river, a momentum correction factor is used in the convective acceleration term of the momentum equation, shown below:

$$\frac{\partial Q}{\partial t} + \beta \frac{\partial}{\partial x}(Qu) + gA\frac{\partial h}{\partial x} = gA(S_0 - S_{E/C} - S_f) + M_L . \tag{4.23}$$

v. *Meandering form of natural rivers–the addition of a sinuousity factor*

In nature, rivers flow in meandering, curving paths instead of the prismatic, straight pathways that scientists and researchers study. This meandering must be reflected in the Saint-Venant equations, so sinuosity factors are introduced mathematically into the continuity and momentum equations. The sinuosity coefficient, used in the calculation of the sinuosity factor, is the ratio of the straight and real distances between two nodes along the river. The continuity equation area of each reach is calculated with and without using this coefficient, and their ratio is set to S_c.

For the momentum equation, the ratio of conveyances calculated with the real and straight distance between nodes is used to calculate the sinuosity factor S_m. Using the

sinuosity factors and converting the velocity terms into flow terms so that only two unknowns remain, the modified version of the continuity equation of the Saint-Venant equations becomes

$$\frac{\partial s_c (A + A_0)}{\partial t} + \frac{\partial Q}{\partial x} - q_L = 0\,, \tag{4.24}$$

and the momentum equation becomes

$$\frac{\partial s_m Q}{\partial t} + \frac{\partial (\beta Q^2 / A)}{\partial x} + gA\left(\frac{\partial h_r}{\partial x} + S_f + S_{ec}\right) + M_L = 0\,. \tag{4.25}$$

With the above mentioned modifications for the natural, meandering rivers, the final form of the Saint Venant equations becomes

$$\frac{\partial s_c (A + A_0)}{\partial t} + \frac{\partial Q}{\partial x} - q_L = 0 \tag{4.26}$$

$$\frac{\partial s_m Q}{\partial t} + \frac{\partial (\beta Q^2 / A)}{\partial x} + gA\left(\frac{\partial h_r}{\partial x} + S_f + S_{ec}\right) + M_L = 0\,. \tag{4.27}$$

4.3. Initial and Boundary Conditions

4.3.1. Initial Conditions

In order to start the solution, the initial values of the unknowns, which are the discharge and water surface elevation, need to be determined along the one-dimensional river reach.

These initial conditions can be obtained from field data, a previous unsteady model solution, or a solution for a steady and non-uniform flow equation. In any of these cases, the initial conditions are given in the following form:

$$Q(x,0) = Q_0(x) \tag{4.28}$$

$$h_r(x,0) = h_{r0}(x)\,, \tag{4.29}$$

where Q_0 [L^3/T] and h_{r0} [L] represent the discharge and water surface elevation in the channel at the start of the simulation, respectively.

4.3.2. Boundary Conditions

Two different types of boundary conditions, external and internal, are located in the domain. External boundary conditions are located at the most upstream and downstream points of the river system and internal boundary conditions at the junctions where another tributary enters the river system. The model proposed in this study is capable of modeling both a network of river channels and a single channel. However, it does not allow for looped channel networks, only tree-like network structures. The tree-like network structure can accommodate more than one upstream boundary condition and a single downstream boundary condition.

4.3.2.1. External Boundary Conditions

At the upstream boundary, only a discharge or stage hydrograph can be used as the boundary condition. At the downstream boundary, some type of rating curve can also be used as a boundary condition in addition to the discharge or stage hydrograph.

The discharge or stage hydrograph at the upstream can be expressed as

$$Q(0,t) = Q_u(t) \tag{4.30}$$

$$h_r(0,t) = h_u(t), \tag{4.31}$$

where Q_u [L^3/T] and h_u [L] are the upstream boundary discharge and water surface elevation values, respectively. In a similar manner, the discharge or stage hydrograph boundary conditions at the downstream point can be expressed as

$$Q(L_d,t) = Q_d(t) \tag{4.32}$$

$$h_r(L_d,t) = h_d(t), \tag{4.33}$$

where Q_d [L^3/T] and h_d [L] are downstream boundary discharge and water surface elevation values, respectively, and L_d [L] is the total length of the system of rivers.

The downstream boundary condition can be defined as a rating curve as well. Three different types of rating curves can be used as a boundary condition. A single-valued rating curve uses a stage-discharge data set and linear interpolation, as shown below:

$$Q(L_d,t) = Q^k + \frac{Q^{k+1} - Q^k}{h_r^{k+1} - h_r^k}(h_d - h_r^k), \tag{4.34}$$

where Q^k [L^3/T], Q^{k+1} [L^3/T], h_r^k [L] and h_r^{k+1} [L] are tabular data sets of the discharge and stage values consecutively on the rating curve and h_d [L] is the stage at the downstream boundary.

A looped rating curve describes the stage value according to several possible discharge values, depending on the hydraulic conditions of the channel. It can be expressed using Manning's equation:

$$Q(L_d,t) = \frac{c_1}{n_r} A R_h^{2/3} S_f^{1/2}, \tag{4.35}$$

where the friction slope S_f is derived from the modified momentum equation as

$$S_f = -\frac{1}{gA}\frac{\partial Q}{\partial t} - \frac{1}{gA}\frac{\partial (Q^2/A)}{\partial x} - \frac{\partial h_r}{\partial x}. \tag{4.36}$$

Critical depth can also be used as the downstream boundary condition when the most downstream point of the modeling domain is a controlling structure such as a weir. In such a case, the critical depth is defined by the critical discharge:

$$Q(L_d, t) = \sqrt{\frac{g}{W}} A^{3/2}, \tag{4.37}$$

where W is the cross-sectional top width of the channel.

4.3.2.2. Internal Boundary Conditions

At the junctions where two or more rivers intersect in a river network, internal boundary conditions must satisfy the mass and energy balance. The water depth has to be equated at each of the rivers coming into or out of the junction through the mass balance equation. The mass balance equation at a junction is given as

$$\sum_{k=1}^{m} Q_k - Q_0 = \frac{dS}{dt}, \tag{4.38}$$

where m is the total number of rivers entering the junction. Only one outgoing river from the junction is allowed in this model. Q_k [L^3/T] is the discharge at the end of the k^{th} inflowing river into the junction; Q_0 [L^3/T] represents the discharge at the beginning of the outflowing river from the junction. dS/dt [M/T] denotes the change in the storage of mass within the junction. The change in storage is believed to be negligible with respect

to the change in storage within a river (Fread 1976; Gunduz 2004). Hence, the mass balance equation becomes a continuity equation. The energy conservation equation at the junction can be written as

$$(h_r)_k + \frac{V_k^2}{2g} = (h_r)_0 + \frac{V_o^2}{2g} + h_T \quad k = 1, 2, ..., m\,, \tag{4.39}$$

where $(h_r)_k$ [L] and V_k [L/T] are the stage and flow velocity at the end of the kth inflowing channel into the junction, respectively, and $(h_r)_0$ and V_o are the stage and flow velocity at the beginning of the outflowing channel from the junction, respectively. h_T [L] is the total head loss in the junction. In the case in which all the flows associated with one junction are subcritical and the head loss in the junction is negligible, Equation (4.39) simplifies to

$$(h_r)_k = (h_r)_0 \quad k = 1, 2, ..., m\,, \tag{4.40}$$

which is commonly used in the modeling of river networks (Fread 1976; Gunduz 2004).

4.4 Numerical Solution Scheme–The Preissmann Weighted Four-Point Scheme

These two equations together form the system of equations representing unsteady flow in channels, also known as the Saint-Venant equations. These two equations are coupled, nonlinear, first-order partial differential equations of the hyperbolic type whose solutions

require one initial and two boundary conditions (Baltas 1988). These equations have no analytical solution except for a few special cases (Gunduz and Aral 2004). However, several numerical methods that solve Saint-Venant equations have been developed. They can be classified into i) the method of characteristics, ii) the method of finite differences, and iii) the method of finite elements. Each of these methods can further be classified as explicit or implicit, depending on the solution.

Among these three numerical solution procedures, the method of finite elements is less likely to be selected to solve the Saint-Venant equations of unsteady flow (Blandford and Ormsbee 1993; Cooley and Moin 1976; Szymkiewicz 1991). Even though method of finite elements offers many advantages over other numerical solution procedures in a general setting, these advantages become somewhat less viable in a one-dimensional setting such as rivers. The power of the finite element method is much more apparent in two- and three-dimensional problems.

The method of characteristics has been the first technique successfully applied to solving Saint-Venant equations. The application of this method requires the transformation of the original partial differential equations into their characteristic forms, thus having ordinary differential equations, which are easier to deal with. Liggett and Woolhiser (1967) and Streeter and Wylie (1967) developed explicit solution techniques to characteristic forms of the Saint-Venant equations while Amein (1966) and Wylie (1970) formulated some implicit solution methods for the same characteristic forms of the original equations.

The method of characteristics is applied to either a characteristic (curvilinear) grid, which is not suitable for natural pathways with irregular geometry, or to a rectangular grid in the x-t solution plane, which requires interpolation within a finite difference solution procedure (Fread 1985; Gunduz 2004). These restrictions limit the application of the method of characteristics to flood routing (Fread 1985).

The method of finite differences involves the transformation of the governing differential equations into algebraic equations through approximation of the derivative in terms of difference equations. Using an explicit finite difference method, the solution is advanced from point to point along one time line until all the unknown values in that particular time line have been calculated. Afterwards, the same principle is applied in the next time step. In an implicit finite difference method, the solution from one time line to the next is performed simultaneously on all the points of unknown values. Explicit methods are straightforward and easily programmed, but they are restricted by conditions for stability. However, the solution of implicit methods is more complex and difficult to program, but most are unconditionally stable (Fread 1985).

The first explicit technique for the solution of flood routing problems was developed by Stoker in 1953, followed by Liggett and Woolhiser in 1967 and later by Strelkoff in 1970. The restrictions inflicted on the size of the computational time step by explicit methods drove the need to develop implicit methods, which were first formulated by Preismann in 1961 and followed by the work of Amein and Chu in 1975. Amein and

Fang (1969) showed that implicit schemes are the only ones suited to handling large variations in flow characteristics. Today, the Preismann method has become the most implemented method due to its flexibility in using large time steps and its unconditional stability (Gunduz 2004). The numerical grid for this method is below:

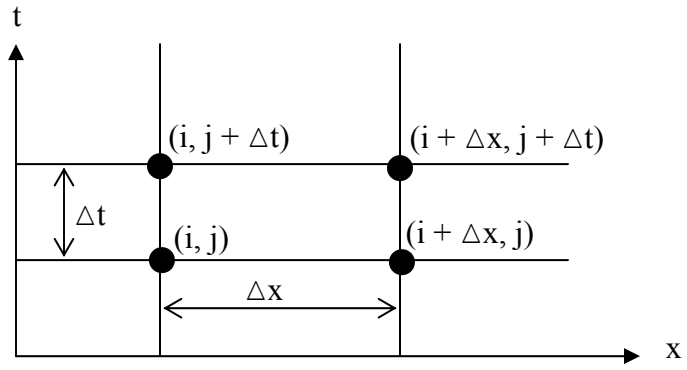

Figure 4.5 The numerical grid for the weighted four-point scheme.

The Preissmann four-point method is weighted implicitly at each time level and unconditionally stable for weighing factor θ between 0.5 and 1.0. It permits the use of unequal space and time steps. This scheme has second-order accuracy when θ is 0.5 and first-order accuracy when θ is 1.0.

If ϕ is a variable that changes with respect to time and space, the finite difference representation is the average of the forward difference in time between four corners given as

$$\frac{\partial \phi}{\partial t} = \frac{\left(\frac{\phi_x^{t+\Delta t} + \phi_{x+\Delta x}^{t+\Delta t}}{2} - \frac{\phi_x^t + \phi_{x+\Delta x}^t}{2} \right)}{\Delta t} \tag{4.41}$$

$$\frac{\partial \phi}{\partial x} = \frac{(1-\theta)\left(\phi^{t}_{x+\Delta x} - \phi^{t}_{x}\right) + \theta\left(\phi^{t+\Delta t}_{x+\Delta x} - \phi^{t+\Delta t}_{x}\right)}{\Delta x}, \tag{4.42}$$

and the ϕ itself can be represented using a similar finite difference representation:

$$\phi = (1-\theta)\left(\frac{\phi^{t}_{x+\Delta x} + \phi^{t}_{x}}{2}\right) + \theta\left(\frac{\phi^{t+\Delta t}_{x+\Delta x} + \phi^{t+\Delta t}_{x}}{2}\right). \tag{4.43}$$

With Equations (4.42) to (4.43) as guidelines, both the continuity and momentum equations can be written in terms of these representations. Thus, the finite difference representation of the continuity equation becomes

$$\begin{aligned}
&\frac{\Delta x_i}{2\Delta t^{j}}\left[s^{j+1}_{c_{i+1/2}} (A + A_0)^{j+1}_{i+1} + s^{j}_{c_{i+1/2}} (A + A_0)^{j+1}_{i} - s^{j}_{c_{i+1/2}} (A + A_0)^{j}_{i+1} - s^{j}_{c_{i+1/2}} (A + A_0)^{j}_{i} \right] \\
&+\theta_f \left[Q^{j+1}_{i+1} - Q^{j+1}_{i} - \Delta x_i \left[\left(-\frac{K_r w_r}{m_r} \right)^{j+1}_{i+1/2} \left(h^{j+1}_{r_{i+1/2}} - h^{j+1}_{g_{i+1/2}} \right) \right] - \Delta x_i (q_{L2})^{j+1}_{i+1/2} \right] \\
&+(1-\theta_f) \left[Q^{j}_{i+1} - Q^{j}_{i} - \Delta x_i \left[\left(-\frac{K_r w_r}{m_r} \right)^{j}_{i+1/2} \left(h^{j}_{r_{i+1/2}} - h^{j}_{g_{i+1/2}} \right) \right] - \Delta x_i (q_{L2})^{j}_{i+1/2} \right] = 0
\end{aligned} \tag{4.44}$$

Similarly, the momentum equation can be written as

$$\frac{\Delta x_i}{2\Delta t^j}\left[s^{j+1}_{m_{i+1/2}} Q^{j+1}_{i+1} + s^{j}_{m_{i+1/2}} Q^{j+1}_{i} - s^{j}_{m_{i+1/2}} Q^{j}_{i+1} - s^{j}_{m_{i+1/2}} Q^{j}_{i} \right]$$
$$+\theta_f \left[\begin{array}{l} (\beta Q^2 / A)^{j+1}_{i+1} - (\beta Q^2 / A)^{j+1}_{i} + g A^{j+1}_{i+1/2}\left[h^{j+1}_{r_{i+1}} - h^{j+1}_{r_i} + \Delta x_i S^{j+1}_{f_{i+1/2}} + \Delta x_i S^{j+1}_{ec_{i+1/2}} \right] \\ +\Delta x_i (M_{L1})^{j+1}_{i+1/2} + \Delta x_i (M_{L2})^{j+1}_{i+1/2} \end{array} \right] \quad . \quad (4.45)$$
$$+(1-\theta_f) \left[\begin{array}{l} (\beta Q^2 / A)^{j}_{i+1} - (\beta Q^2 / A)^{j}_{i} + g A^{j}_{i+1/2}\left[h^{j}_{r_{i+1}} - h^{j}_{r_i} + \Delta x_i S^{j}_{f_{i+1/2}} + \Delta x_i S^{j}_{ec_{i+1/2}} \right] \\ +\Delta x_i (M_{L1})^{j}_{i+1/2} + \Delta x_i (M_{L2})^{j}_{i+1/2} \end{array} \right] = 0$$

The definitions developed for the slope terms S_f and S_{ec}, and the lateral flow terms M_{L1} and M_{L2} are included in the above representation. Subscripts *i* and *j* represent the spatial and temporal indices, respectively. The terms with subscript j are known either from initial conditions or from the solution of the Saint-Venant equations at the previous time line. As the cross-sectional area and the top width of the river are functions of water surface elevation, the only unknown terms in these equations are the discharge and water surface elevation at the $(j+1)^{th}$ time line at nodes *(i)* and *(i+1)*. Therefore, these equations contain only four unknowns. The remaining terms are either known constants or functions of the unknowns. The algebraic equations (4.44) and (4.45) are nonlinear, requiring an iterative solution technique.

When the system is derived using the above guidelines, 2(N-1) equations are formed for one time-line between the upstream and downstream boundaries of a channel of N nodes. At this point, there are 2N unknowns for each time line with 2(N-1) equations to solve them. Hence, two more equations are needed to close the system and solve it. These two equations are supplied by the upstream and downstream boundary conditions of the channel. The system of 2N equations with 2N unknowns is non-linear and solved by a matrix solution algorithm.

To demonstrate the solution of scheme, two functions, F and G, can be defined as F being the residual of the continuity equation, and G being the residual of the momentum equation. Both F and G are functions of four dependent variables, S_1, S_2, S_3, and S_4 which represent the to represent the unknowns, $Q_x^{t+\Delta t}$, $A_x^{t+\Delta t}$, Q_x^t, and A_x^t, respectively, which are the flow and area at the present and future time steps.

This solution matrix is formed by the application of Taylor's series for these two equations, F and G as follows:

$$F(S_1, S_2, S_3, S_4) = 0 \tag{4.47}$$

$$G(S_1, S_2, S_3, S_4) = 0\,. \tag{4.48}$$

If the exact solution to the unknows were known as $S_{1,r}$, $S_{2,r}$, $S_{3,r}$, and $S_{4,r}$ as

$$\begin{aligned} S_1 &= S_{1,r} \\ S_2 &= S_{2,r} \\ S_3 &= S_{3,r} \\ S_4 &= S_{4,r} \end{aligned}\quad, \tag{4.49}$$

then the exact solution can be approximated by the following equation using Taylor's series expansion:

$$F(S_{1,r}, S_{2,r}, S_{3,r}, S_{4,r}) \approx F(S_{1,\xi}, S_{2,\xi}, S_{3,\xi}, S_{4,\xi}) + \frac{\partial F}{\partial S_1} dS_1\Big|_{\xi} + \frac{\partial F}{\partial S_2} dS_2\Big|_{\xi} + \frac{\partial F}{\partial S_3} dS_3\Big|_{\xi} + \frac{\partial F}{\partial S_4} dS_4\Big|_{\xi} = 0 \tag{4.50}$$

and

$$G(S_{1,r}, S_{2,r}, S_{3,r}, S_{4,r}) \approx G(S_{1,\xi}, S_{2,\xi}, S_{3,\xi}, S_{4,\xi}) + \frac{\partial G}{\partial S_1} dS_1\Big|_{\xi} + \frac{\partial G}{\partial S_2} dS_2\Big|_{\xi} + \frac{\partial G}{\partial S_3} dS_3\Big|_{\xi} + \frac{\partial G}{\partial S_4} dS_4\Big|_{\xi} = 0, \tag{4.51}$$

where the higher-order terms of the Taylor's series expansion can be neglected. Then the solution can be approximated by

$$\begin{aligned} S_{1,r} &\approx S_{1,\xi} + dS_1 \\ S_{2,r} &\approx S_{2,\xi} + dS_2 \\ S_{3,r} &\approx S_{3,\xi} + dS_3 \\ S_{4,r} &\approx S_{4,\xi} + dS_4 \end{aligned}. \tag{4.52}$$

The Equation (4.52) is only an approximate of the true solution; however, this approximation can be improved through iterations in which each interation estimates a solution better than the previous one until there is not much room for improvement (a preset tolerance value can determine this condition):

$$\begin{aligned} S_1^{\xi+1} &\approx S_1^{\xi} + dS_1^{\xi} \\ S_2^{\xi+1} &\approx S_2^{\xi} + dS_2^{\xi} \\ S_3^{\xi+1} &\approx S_3^{\xi} + dS_3^{\xi} \\ S_4^{\xi+1} &\approx S_4^{\xi} + dS_4^{\xi} \end{aligned} \tag{4.53}$$

The estimates from a previous iteration improve with each step further in time and finally converge on a solution, which can be performed by setting the equations in matrix form:

$$\mathbf{J}(X^{\xi})\Delta X = -\mathbf{R}(X^{\xi}), \tag{4.54}$$

where X^{ξ} is a vector of estimated values of the unknowns from the ξ^{th} step or iteration, and the coefficient matrix $\mathbf{J}(X^{\xi})$, also known as the Jacobian, contains the partial derivatives with the values evaluated at the ξ^{th} iteration. ΔX is a vector of unknowns (dS_1, …, dS_4), as given in this example. $\mathbf{R}(X^{\xi})$ is a vector of residuals, the values of which should approach zero as the solution converges to an exact solution. The solution can be obtained using one of the various numerical methods such as Gauss Elimination or LU decomposition for the simultaneous solution of the given equations.

The Jacobian matrix, made up of the partial derivatives of the continuity and momentum equation, must be set up to start the solution. The resulting matrix form is given as

$$\begin{bmatrix}
\frac{\partial G_0}{\partial A_1} & \frac{\partial G_0}{\partial Q_1} & 0 & 0 & 0 & 0 & 0 & . & . & . & 0 & 0 \\
\frac{\partial F_1}{\partial A_1} & \frac{\partial F_1}{\partial Q_1} & \frac{\partial F_1}{\partial A_2} & \frac{\partial F_1}{\partial Q_2} & 0 & 0 & 0 & . & . & . & 0 & 0 \\
. & . & . & . & . & . & . & . & . & . & . & . \\
. & . & . & . & . & . & . & . & . & . & . & . \\
. & . & . & . & . & . & . & . & . & . & . & . \\
0 & . & . & . & \frac{\partial F_i}{\partial A_i} & \frac{\partial F_i}{\partial Q_i} & \frac{\partial F_i}{\partial A_{i+1}} & \frac{\partial F_i}{\partial Q_{i+1}} & . & . & . & 0 \\
0 & . & . & . & \frac{\partial G_i}{\partial A_i} & \frac{\partial G_i}{\partial Q_i} & \frac{\partial G_i}{\partial A_{i+1}} & \frac{\partial G_i}{\partial Q_{i+1}} & . & . & . & 0 \\
. & . & . & . & . & . & . & . & . & . & . & . \\
. & . & . & . & . & . & . & . & . & . & . & . \\
. & . & . & . & . & . & . & . & . & . & . & . \\
0 & 0 & . & . & . & 0 & 0 & 0 & \frac{\partial G_{N-1}}{\partial A_{N-1}} & \frac{\partial G_{N-1}}{\partial Q_{N-1}} & \frac{\partial G_{N-1}}{\partial A_N} & \frac{\partial G_{N-1}}{\partial Q_N} \\
0 & 0 & . & . & . & 0 & 0 & 0 & 0 & 0 & \frac{\partial G_N}{\partial A_N} & \frac{\partial G_N}{\partial Q_N}
\end{bmatrix}_{NxN}
\begin{bmatrix}
dA_1^{\xi} \\ dQ_1^{\xi} \\ dA_2^{\xi} \\ dQ_2^{\xi} \\ . \\ . \\ . \\ dQ_{N-2}^{\xi} \\ dA_{N-1}^{\xi} \\ dQ_{N-1}^{\xi} \\ dA_N^{\xi} \\ dQ_N^{\xi}
\end{bmatrix}_{Nx1}
=
\begin{bmatrix}
R_{2,0}^{\xi} \\ R_{1,1}^{\xi} \\ R_{2,1}^{\xi} \\ R_{1,2}^{\xi} \\ . \\ . \\ . \\ R_{2,N-2}^{\xi} \\ R_{2,N-2}^{\xi} \\ R_{1,N-1}^{\xi} \\ R_{2,N-1}^{\xi} \\ R_{2,N}^{\xi}
\end{bmatrix}_{Nx1} \quad (4.55)$$

When all the equations are written for a system with N_k number of nodes, $2(N_k\text{-}1)$ equations are formed for one time-line between the upstream and downstream boundaries of channel k. At this point, we have $2N_k$ unknowns for each time line with $2(N_k\text{-}1)$ equations to solve them. Hence, we need two more equations to close the system and solve it. These two equations are supplied by the upstream and downstream boundary conditions of the channel. When this procedure is repeated for each river tributary in the network, a total of $\sum(2N_k) = 2N$ equations are formed. k is the number of rivers in the network, and N is the total number of nodes in the entire system. The system of 2N equations with 2N unknowns is non-linear and solved by the matrix solution algorithm explained above.

Newton-Raphson is the most common iterative technique used for solving a system of non-linear equations. When a sufficiently accurate first estimate is provided, the Newton-

Raphson method converges efficiently to a root. The basic steps in this solution follow (EnvironmentalLaboratory 1995):

1. Assume Q and A are known from either of the previous time steps of the initial conditions.
2. Insert Q and A into the equations for F and G and form the first vector of residuals by evaluating the continuity and momentum equations.
3. After the residuals are formed, the gradients should be formed and the estimates used to calculate the residuals (either the initial conditions or the estimates obtained from the previous iteration)
4. Using the matrix form, solve the system of equations.
5. The ΔX^{ξ}, the solution of the matrix form, is the departure vector from the old estimates. Using this departure vector, evaluate new estimates:

$$\begin{aligned} Q_x^{t+\Delta t,\xi+1} &= Q_x^{t+\Delta t,\xi} + dQ_x^{\xi} \\ A_x^{t+\Delta t,\xi+1} &= A_x^{t+\Delta t,\xi} + dA_x^{\xi} \end{aligned} \tag{4.56}$$

6. Check to see how close the new estimates match the previous ones. If the new estimates are within some specified tolerance, then proceed to the next time step beginning at step 1. If they are not within the specified tolerance, repeat the process beginning at step 2.

4.5 Verification of the Hydrodynamics Solution

The solution procedure has been applied to some simple hypothetical cases for testing and verification purposes. These example applications are also used to verify the solution technique used in this thesis. In Figure 4.6 below, one of these example cases is depicted. The set of non-linear, coupled partial differential equations, which comprise the so-called Saint Venant equations, are applied to a single, trapezoidal channel that is 10 km long with a bed slope of 0.001 m/m and a Manning roughness coefficient of 0.020. The sides of the trapezoidal cross-section of the channel, with a width of 20 m., have a 2:1 ratio

A triangular hydrograph is used as the upper boundary condition, and a constant depth of 1.44 m is used as the downstream boundary condition.

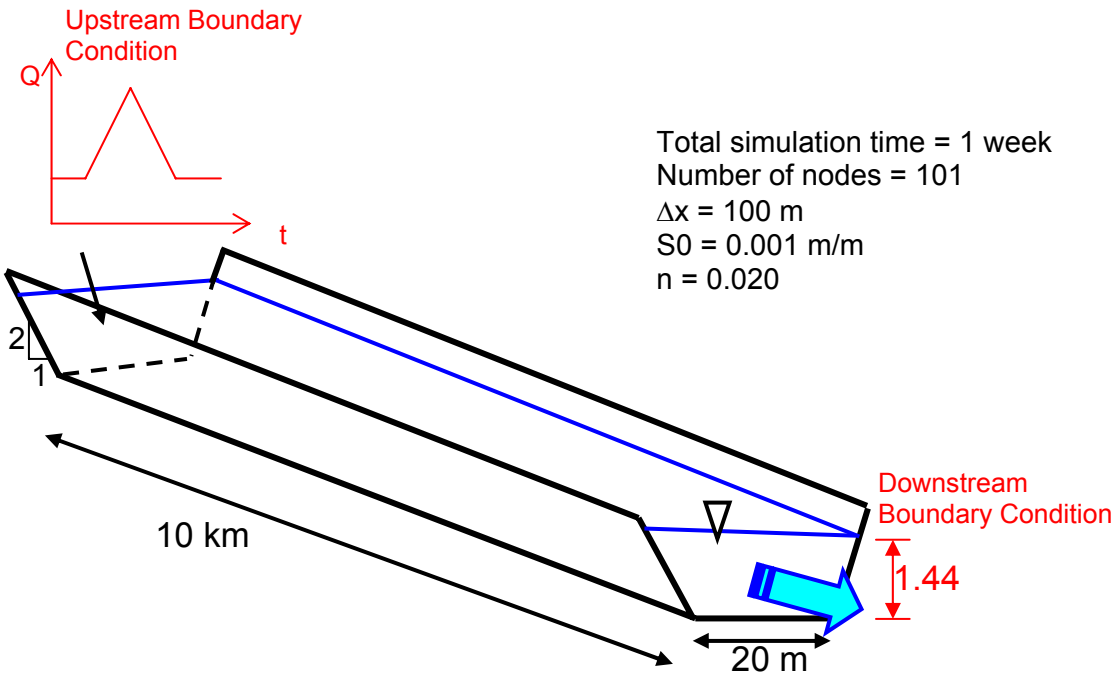

Figure 4.6 A schematic view of a single, trapezoidal channel

HEC-RAS, a well-known and widely-used flood routing model developed by the USGS is used to verify the model developed in this study. Different example cases are used for comparison between the model in this study and HEC-RAS, Figures 4.7 and 4.8 below show the results from the application of the single, trapezoidal channel explained above.

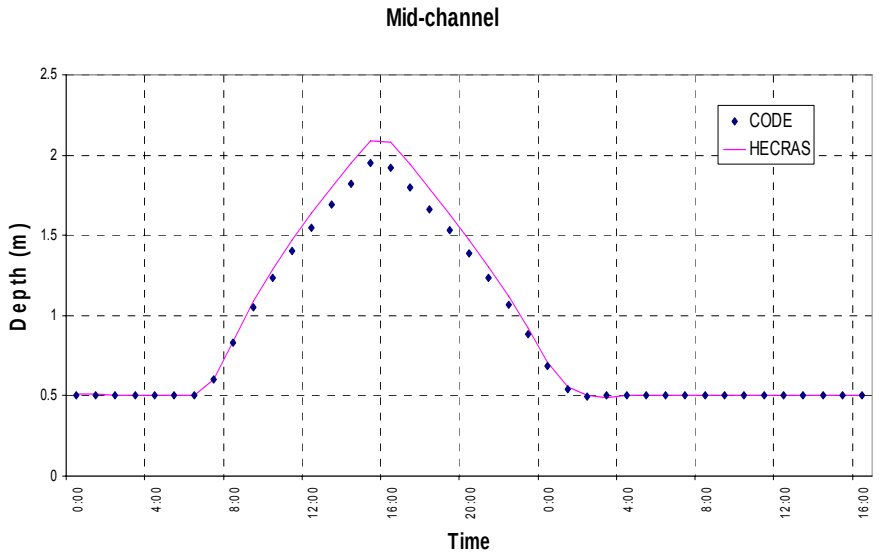

Figure 4.7 A comparison between this model and HEC-RAS at mid-channel

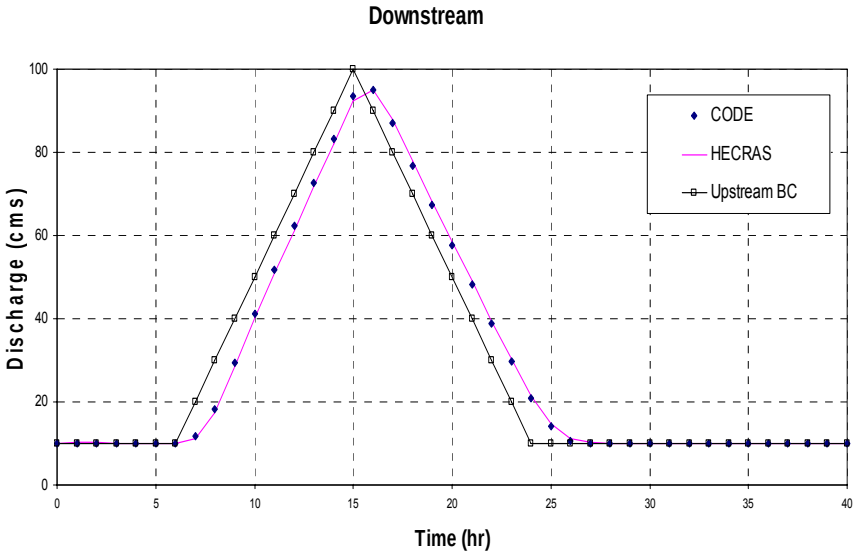

Figure 4.8 A comparison between this model and HEC-RAS at the downstream boundary condition.

Based on the results from both the model described and developed in this study and HEC-RAS, which has been run under the same conditions, the developed model, these figures exhibit confidence in the developed model.

4.6. Channel Network Example

A second example application involves the existence of a junction and more than one channel entering the junction. In this example case, straight, trapezoidal channels make up the configuration given in Figure 4.9 below

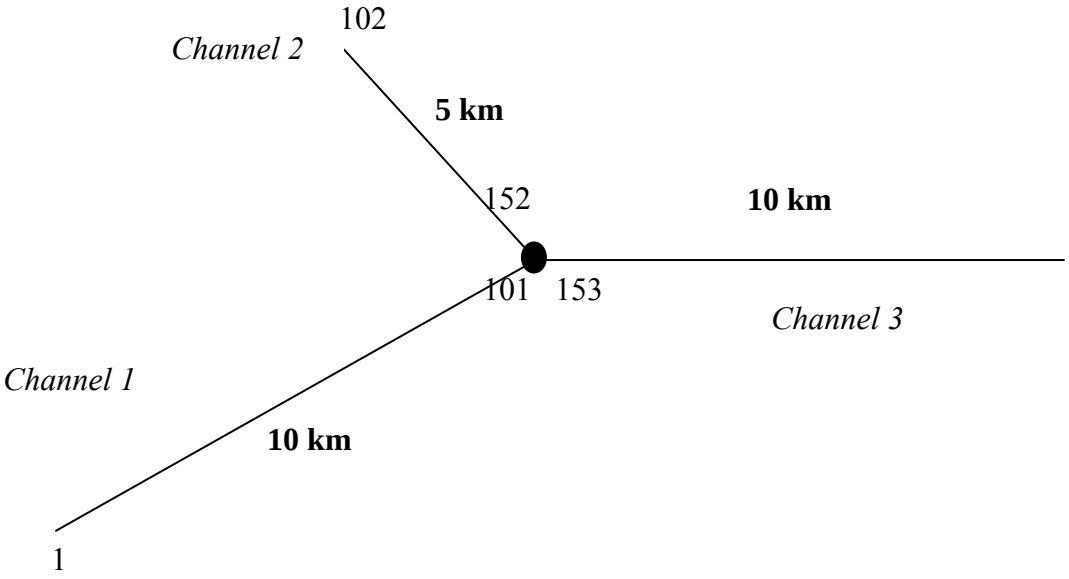

Figure 4.9 An example river network

In this case of a river network application, a total of three rivers with one junction is examined. Two of the rivers enter the junction while a third one exits. The figure (which figure), which illustrates the set up of the river network, shows that the two rivers are 10 km long and 5 km long. All the nodes are separated by 100 m with a total of 253 nodes in the system. The figure also depicts the node numbers at the beginning and end of each river channel.

All the rivers have a constant bed slope of 0.001 m/m and a Mannings' roughness coefficient of 0.030 in the main channel. The cross-sections of all three rivers are trapezoids with a 10 m bottom width and side slopes of a 2:1 ratio. No lateral overland or seepage flow occurs. The total length of the run was for 50 hours at one-hour intervals.

The upstream boundary condition for the 5 km river is a discharge time series composed of two sequential triangular hydrographs, and the upstream boundary condition for the 10 km river entering the junction is a triangular discharge hydrograph. The downstream condition of the outflowing river is a depth of 2 m.

The results of the application of the same model to a river system network are presented in Figure 4.10 below. Channel 1, a triangular hydrograph, and Channel 2, a double triangular hydrograph, form a confluence at the junction and combine their flow patterns. This new flood pattern is routed in Channel 3, which has a 2 m constant depth downstream boundary condition.

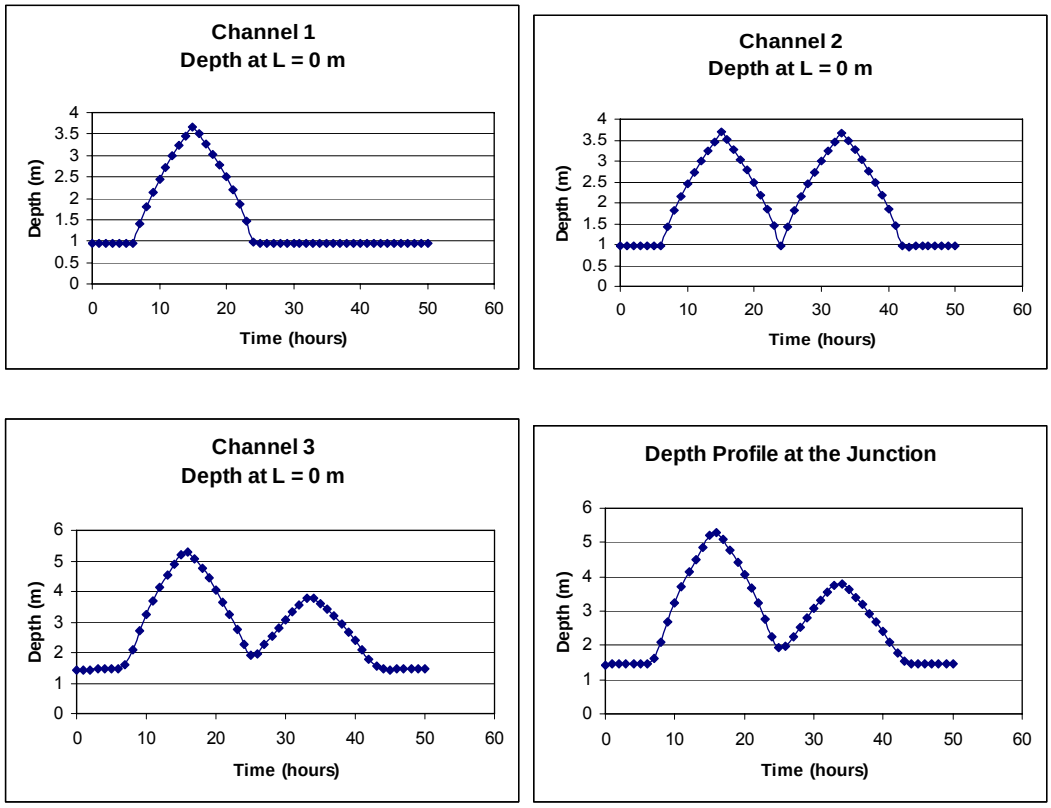

Figure 4.10 Results of a river network application

4.7 Altamaha River Application

The Lower Altamaha River basin, formed by the confluence of the Ocmulgee and Oconee Rivers, is the largest watershed in Georgia. The confluence of the two rivers then forms the Altamaha River, which flows into the Atlantic Ocean about 137 miles from the confluence. Approximately 100,000 gallons of fresh water per second is expelled into the Atlantic Ocean from this system, which is home to 120 species of rare or endangered plants and animals. A plan view of the Altamaha River system can be seen in Figure 4.11 below.

Figure 4.11 The Altamaha River system

In order to model the river network, a simplified, conceptual version of the network is depicted in Figure 4.12 below. This version illustrates the differences in the real versus linear length between the upstream and the downstream of the channels, with real distances in blue and linear distances in black. These values are used to calculate the sinuosity factors of the rivers, which help modify the model for the meandering nature of rivers. The three channels in the Altamaha River network are called Altamaha River Main 1, Altamaha River Main 2, and the Ohopee River, which acts as a tributary entering the main stream divided by this junction. The channels are divided into small reaches at 394 cross-sections. The required data at these nodes are obtained by using measurements taken at three gaging stations by USGS, and the topographic maps of the region. Each node corresponds to a USGS gage, so geometric information as well as the flow and water elevation at the start of the model is known. The geometric information, which is actually the depth versus width information at each node, is known from the gages and entered into the model. One such cross-section is shown in Figure 4.13 below. For the

application of this model, each cross-section if described with 10 sets of elevation-top width pairs.

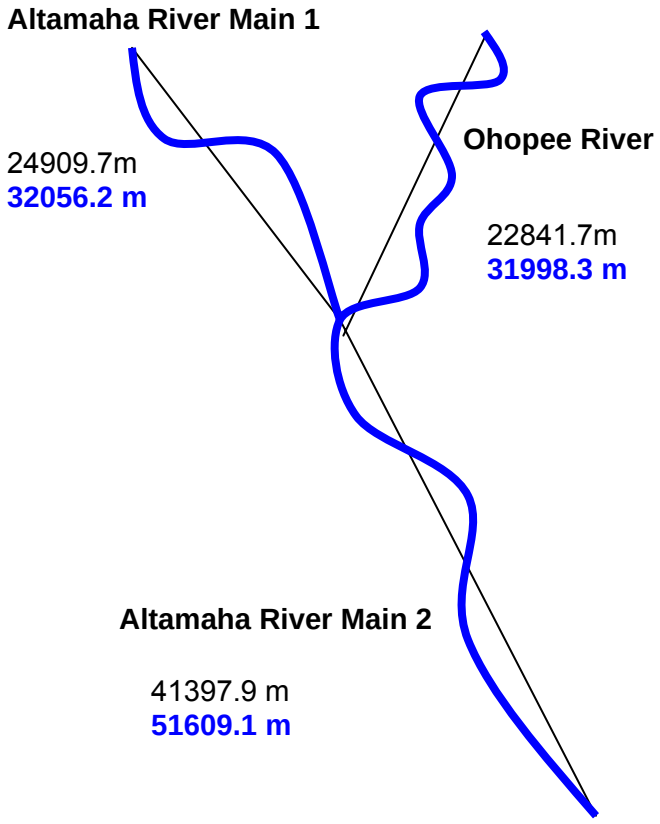

Figure 4.12 Conceptual drawing of the Altamaha River network

From previous modeling studies in the same area, Manning's roughness coefficients have been selected and have values between 0.020 to 0.030 within the main channel and 0.030 to 0.070 along the floodplain (Gunduz and Aral 2004).

Three boundary conditions are specified for the application of Altamaha River system for the river flow model. The upstream boundary conditions at both the Altamaha River as well as Ohoopee River is taken to be discharge-time series obtained from Baxley and Reidsville river stream gages operated by U.S. Geological Survey. The most downstream boundary condition is a rating curve obtained from the Doctortown gauging station, developed by the U.S. Geological Survey staff for use in their modeling studies.

The initial discharge and stage conditions in the river network are based on previous studies in the same domain (Gunduz and Aral 2004).

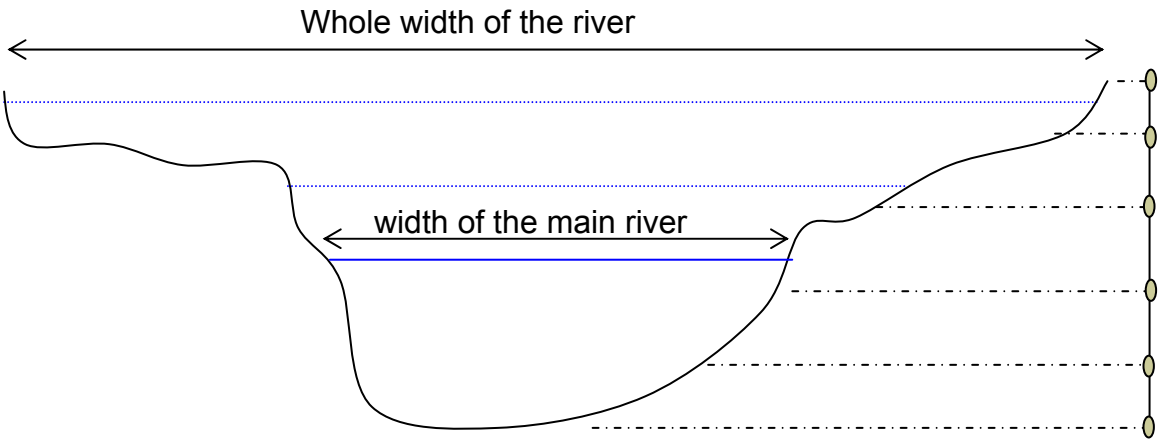

Figure 4.13 Cross section view of a node.

The results of the Altamaha River applications will be used directly and indirectly as input for the contaminant transport model, which will be explained in detail in the next chapter. The results of this application include a velocity distribution in the river network over the simulation time as well as depth and width values at each node at each time step.

Width is used to calculate the surface area of each element together with the distance between nodes. Depth will then be used to calculate the volume of water in each element using the previously calculated surface area information. Velocities at each node will be used in the advection portion of the contaminant transport equation as well as in the calculation of a longitudinal dispersion coefficient for each element, using an empirical formula. All these results will be prepared as an array input in a small program developed to handle output and then to use the output of the hydrodynamic portion and convert it into input files to be used by the contaminant transport model.

As these results are intermediate steps in the solution of totally dynamic fugacity-based water quality model, they are not shown here. Just as an example, the velocity distribution in the Altamaha River network is given below:

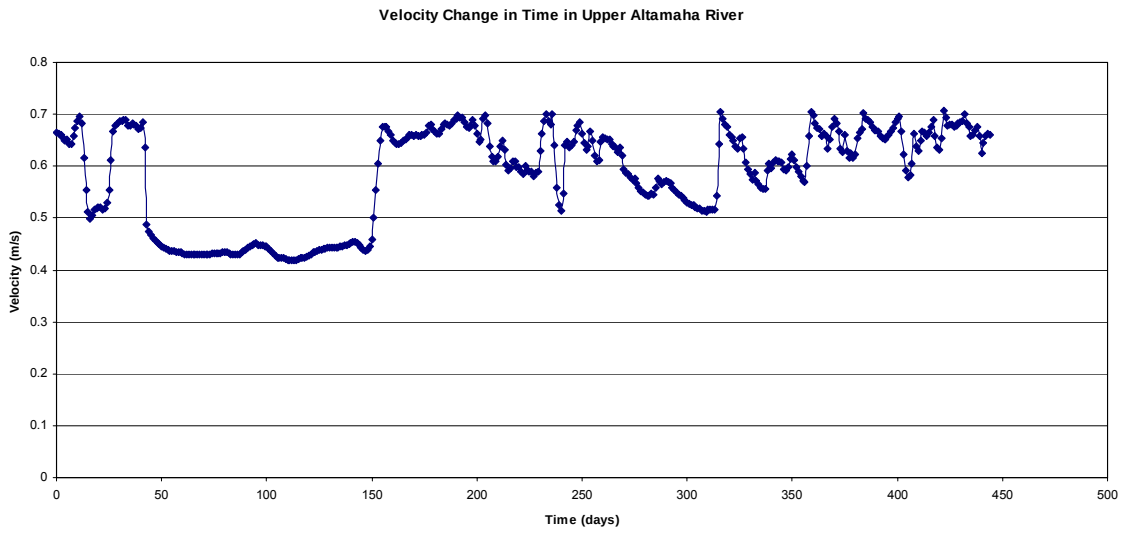

Figure 4.14 Velocity time series at location 5 km from upstream in the Altamaha River system

The velocity distribution follows the rise and fall of water levels due to rain events, water intake, and other activities performed in a channel, so it does not follow a smooth curve. The real USGS stream gage readings are input into the solution of the model as initial and boundary conditions, and the results reflect changes in the river elevations and flow rate fluctuations due to natural and artificial reasons. The velocity time series is illustrated in Figure 4.14 and the width and depth distribution at each cross-section are used as input information into the contaminant transport model developed in Chapter 5.